Frequenz
63 (2009)
9–10

Investigations on a Comb Filter Approach for IR-UWB Systems

Thanawat Thiasiriphet, Mario Leib, Dayang Lin, Bernd Schleicher,
Jürgen Lindner, Wolfgang Menzel and Hermann Schumacher

Abstract – In this article a method to increase the signal to noise ratio (SNR) of an impulse-radio ultra-wideband receiver system is investigated. It uses a comb filter to increase the SNR also in case of multipath propagation, narrowband interference and multiple users or sensors, with the advantage that pulse position modulation with energy detection can be used. In theory 10·log(*N*) dB can be achieved, where *N* is the number of impulses summed up. Simulations with physical hardware components are discussed and a hardware implementation for the frequency range 3.1 – 10.6 GHz is presented.

Index Terms – ultra-wideband, UWB, comb filter, impulse-radio, SNR improvement

1 Introduction

In contrast to carrier-based transmission systems, impulse-radio ultra-wideband (IR-UWB) systems use short sub-nanosecond impulses for a transmission of information. The use of UWB is not only limited to communications, UWB systems can also provide good spatial resolution for localization and sensing applications [1]. UWB impulses are considered to be baseband signals, which can be modulated by varying the amplitude or the position of the impulses themselves. This approach promises low realization complexity. Furthermore, it has the potential to realize transmitters and receivers with pure analogue hardware, therefore omitting "power-hungry" wideband analogue-to-digital-conversion. Hence, systems with a low power consumption can be constructed, which are attractive for many applications, e. g. for medical purposes such as implant communication [2], wireless vital sign (breathing rate, heart rate) detection [3], tissue characterization and medical imaging [4]. In this paper, we propose an UWB system, which can be applied for communication and radar in one system concept.

The UWB system is targeting the frequency spectral mask allocated by the Federal Communication Commission (FCC) [5], since licensed operation is the basis for a commercial use of devices. The concept can also be applied to meet the emerging European ECC UWB regulations with a straightforward modification. The challenges for using UWB come mainly from the low signal power and possibly strong narrow band interference. The idea, which this work follows, is to apply a comb filter with remodulation, which can operate in a multiuser (or multisensor) environment, can deal with narrowband interference and increases the signal to noise ratio (SNR) of the received signal. The receiver concept is shown in Fig. 1, where the comb filter is modelled by a delay element and an adder. The concept can be applied for both, communication and imaging. More about the concept can be found in [6]. A hardware description on the building blocks necessary for a correlation receiver according to Fig. 1 (i. e. a broadband low-noise amplifier, an FCC-compliant impulse generator and an analogue multiplier) can be found in [7].

2 Comb Filter Concept with Spreading Sequence

The comb filter is a feedback loop with an analogue delay and a constant loop gain of one for all frequencies. It is used to perform a coherent combination of the incoming UWB impulses. The feedback loop sums up the number of impulses used for the transmission of a data symbol and is reset after this. For communications, the UWB impulses are modulated with pulse position modulation. Additionally, the impulse train of each data symbol is modulated by a binary spreading sequence, which is needed for multiuser or multisensor separation and contributes to interference cancellation. For sensing applications no modulation of the data symbol is done, but a spreading is applied as well. Transmitted through the channel, the impulses are affected by the channel impulse response. We assume the channel to be time invariant within the symbol period. In the receiver, the signal is first remodulated with the spreading sequence by a biphase modulator. If the spreading sequence matches, all the received impulses have the same weight, if not, the weight is a scrambling of the two sequences. After remodulation the received impulses are summed up by the comb filter. The SNR is significantly improved, since the summation of the signal power grows quadratic, while the noise power grows only linear. Furthermore all interferences are suppressed.

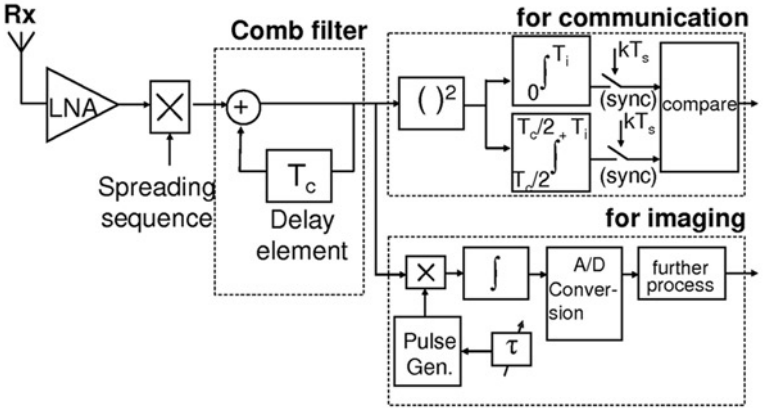

Fig. 1: Receiver structure of the proposed UWB systems including the comb filter approach.

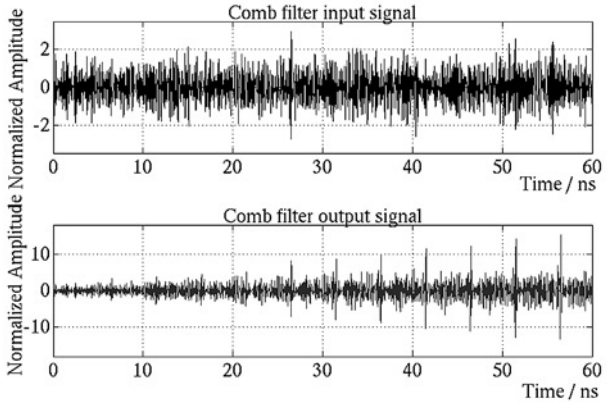

Fig. 2: Comparison between input signal with noise (upper) and accumulated output signal (lower) of a comb filter.

3 Investigations on the Concept

3.1 Simulations with Ideal Components

The comb filter concept is first investigated by simulations with ideal components. For the investigation of the SNR improvement, an AWGN channel is sufficient. A train of modulated UWB impulses and additive noise is the input signal to the multiplier in Fig. 1. The SNR at the input of the multiplier is compared to the SNR after the comb filter to calculate the comb filter processing gain. Fig. 2 shows an example of an input signal with a SNR = -15 dB (upper) compared to the output signal (lower). The SNR improvement can clearly be seen as the receiving impulse becomes visible after a few iterations.

The comb filter processing gain G_p is a function of the gain G_c of the comb filter and the number of iterations N. It can be calculated as

$$G_p = 10 \cdot \log_{10}\left(\left(\sum_{n=0}^{N-1} G_c^n\right)^2 \Big/ \sum_{n=0}^{N-1} G_c^{2\cdot n}\right) \qquad (1)$$

For physical systems this calculation is only valid if no instability is introduced. Therefore the values of G_c can only be in the range of 0–1, because otherwise an oscillation will occur. The maximum processing gain is achieved when G_c is equal to 1. System simulations applying ideal components with a varying loop gain from 0–1 were performed and the results are shown in Fig. 3. The simulation results match perfectly with the mathematical model from (1). As can be seen, higher SNR improvements can be achieved by increasing the number of accumulated impulses, but coming along with a need for a more precise control of the loop gain. Further investigations on the comb filter based energy detector can be found in [6].

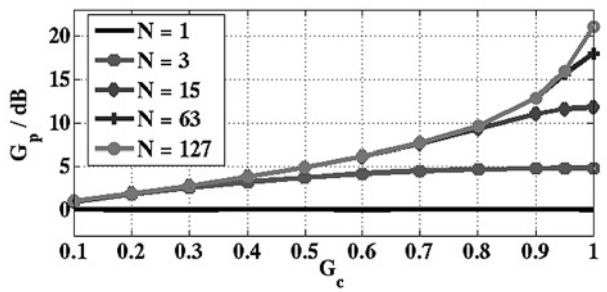

Fig. 3: Simulated SNR improvement G_p versus comb filter gain G_c for N = 1, 3, 15, 63 and 127 impulses

3.2 Simulations with Real Components

Beside simulations based on ideal components, the influence of real components on the comb filter approach is investigated. These simulations were done using the transient solver of the software ADS. For the investigations, the comb filter is implemented using two microstrip-based, multistage UWB 3 dB Wilkinson dividers for power division and combination, an ideal line with a length corresponding to a time delay of 5 ns, and an UWB amplifier within the loop in order to compensate the losses introduced by the power dividers. For the amplifier an available component with a very low group delay variation is chosen [7]. The gain of the amplifier is fixed to 23.5 dB and, hence, an ideal attenuator is connected in the loop to adjust the loop gain to one. For the input signal, a fifth derivative Gaussian impulse with a standard deviation $\sigma = 51$ ps is applied [8]. The impulse repetition rate is set to 200 MHz in accordance with the loop delay.

If the output signal of the comb filter is observed with this configuration, first the amplitude of the output signal increases with each pass, but after some passes a saturation is settling. Comparing the input and the output impulse for 100 cycles (see Fig. 4), a distortion of the impulse shape at the output signal can be seen. This distortion is generated by the gain and phase variations of the components within the loop. Albeit the gain and the group delay of the amplifier is very constant, with a variation of 0.55 dB and 14 ps in the FCC frequency range, these small distortions sum up with each iteration and lead to the saturation effect. In Fig. 4 also a second impulse with reduced amplitude occurs 0.6 ns after the main impulse. This parasitic impulse is caused by reflections at the power dividers.

The determined SNR improvement due to the comb filter for the above described setup is shown in Fig. 5 in comparison to the ideal curve. Due to the saturation effect, a constant SNR of approximately 12 dB is obtained after about 20 cycles. For less loop iterations, the ideal and the simulated curves agree well. The results obtained from this simulation show that an SNR improvement takes place, but depends strongly on the performance of the applied hardware components.

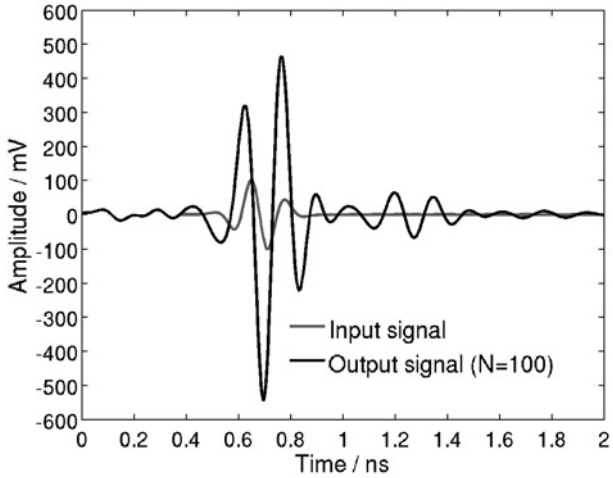

Fig. 4: Input signal compared to output signal of the comb filter for 100 cycles.

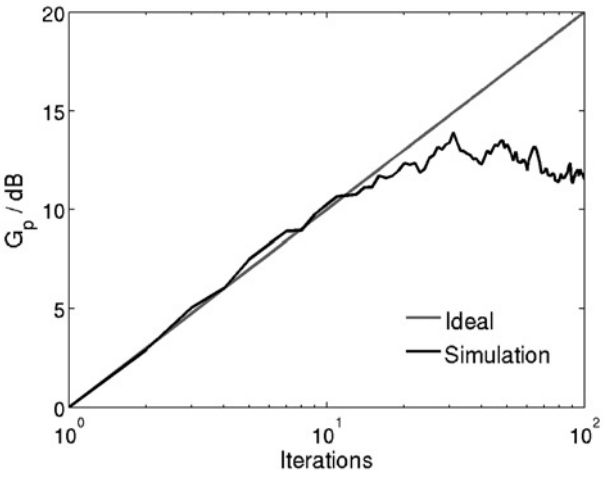

Fig. 5: Simulated SNR improvement versus iterations.

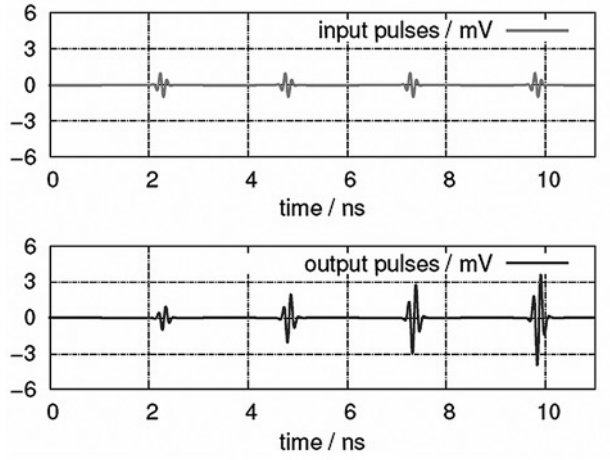

Fig. 7: Transient simulation of the active splitter-combiner circuit fed with fifth Gaussian derivative impulses.

4 Hardware Components for the Comb Filter

4.1 Active Splitter-Combiner Circuit

To incorporate the true time delay in the signal path a splitting node and a summation node are necessary. The summation node combines the impulse energy from the time delay element and the comb filter input, while the splitting node distributes the impulse energy to the time delay element and the output (c. f. Fig. 1). Regarding SNR improvement, the comb filter concept works best with a feedback gain very close to unity. In this approach, an active circuit is investigated, which provides the necessary splitter-combiner operation in a single IC and therefore avoids the occurrence of multiple reflections. A simplified schematic of this active splitter-combiner circuit including the external connected delay element can be seen in Fig. 6. The presented circuit comprises an isolation stage and a stage with a differential pair. The wideband isolation stage has unity gain in the UWB frequency band using a cascode configuration (T1, T2) and a shunt-shunt feedback. It is used to prevent a leakage of signal energy to the stages in front. The isolation stage is capacitively coupled with the input of the differential pair. When the differential pair is fed with impulses at the base connection of transistor T3, these impulses appear inverted at the collector output of transistor T5 and non-inverted at the collector output of transistor T6. With impulses at the base connection of transistor T4, the same transfer takes place, but here the output impulses at T6 are inverted and the output impulses at T5 are non-inverted.

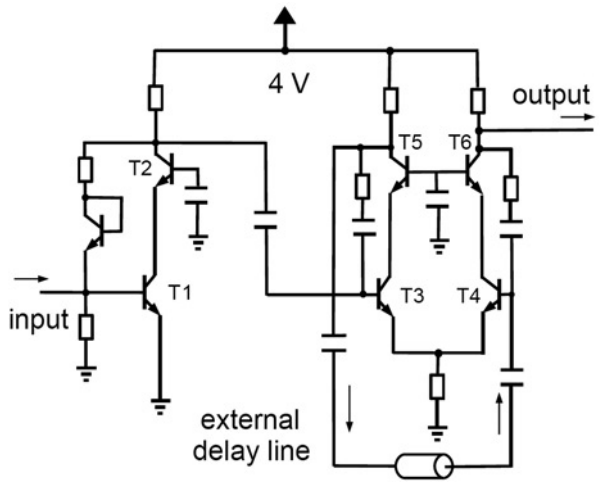

Fig. 6: Simplified circuit schematic of the active comb filter. Biasing not shown here.

The external delay element is connected between the output of transistor T5 and the input of transistor T4, which allows a splitting and combining of impulses with correct alignment. A constructive summation of impulse energy takes place, when the repetition rate of the impulses fits exactly the delay of the delay element. Applying this, the impulses add up from period to period. This can be seen in Fig. 7, where the operation of the circuit is investigated in a transient simulation using real components of a Si/SiGe HBT technology [9] and an ideal delay line. An ideal impulse generator at an elevated repetition rate served as the stimulus for visualization purpose. The cascode differential pair is realized using shunt-shunt feedback to increase the operating frequency range. Intense care was taken to avoid distortion of the impulse shape through gain ripple and group delay variation. Fig. 7 shows that the impulses add up linearly with very small distortions to the impulse shape.

4.2 Triplate Line as True Time Delay

The delay line has to be realized in a compact manner for a practical overall system, but the typical time delay is in the ns range and therefore results in a length of up to several meters. A typical delay is 5 ns corresponding to a maximum achievable data rate of 200 MBit/s. This value is a compromise between a high data rate and a sufficient decay of the channel impulse response. In order to implement a true time delay on a small area, a meander-shaped triplate line is proposed. The triplate line is chosen due to its low dispersive behaviour and the ease of integration with other planar components. A length reduction is achieved using a substrate with a high dielectric constant. For the realization of a 5 ns true time delay test structure, RT6010 with a height of 0.635 mm and a dielectric constant of 10.2 is chosen as substrate base material. The resulting length of 470 mm is implemented on a 42 x 42 mm^2 substrate using 90°-bends and 2.5 mm distance between the inner triplate lines. The realized meander line is displayed in Fig. 8. Vias along the triplate line guarantee the suppression of parasitic parallel plate modes. The via positions are optimized such that the waveguide, formed by the vias and the upper and lower ground metallization, has a cut-off frequency of about 23 GHz. Fig. 9 shows the measured S-parameters of the delay line. There, the return loss including transition from triplate to coaxial line is better than 16 dB. The material losses lead to an increasing insertion loss with increasing frequencies with an insertion loss of 10.3 dB at 10.6 GHz. This loss behaviour needs to be compensated by an

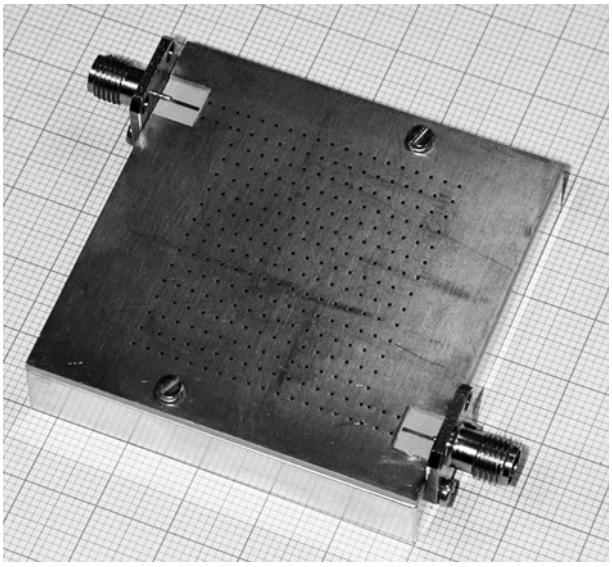

Fig. 8: Realized meander-shaped triplate delay line.

amplifier with optimized frequency response. The group delay of the delay line is 4.92 ns ± 100 ps.

5 Conclusion

Several aspects of a comb filter system with remodulation were presented. The investigations cover ideal simulations, simulations with realistic components and possible improvements to the hardware implementations. Especially the simulations with real components show that an improvement of signal to noise ratio of 12 dB can be achieved and that the performance can be further enhanced by developing custom designed hardware components. For the design of hardware components promising solutions are under construction.

References

[1] R. J. Fontana, "Recent system applications of short-pulse ultra-wideband (UWB) technology", IEEE Trans. on MTT, vol. 52, no. 9, pp. 2087–2104, Sep. 2004.
[2] T. Buchegger, G. Oßberger, A. Reisenzahn, E. Hochmaier, A. Stelzer, and A. Springer, "Ultra- wideband transceivers for cochlear implants," EURASIP Journal on Applied Signal Processing, vol. 18, pp. 3069–3075, Jan. 2005.
[3] M. Leib, E. Schmitt, A. Gronau, J. Dederer, B. Schleicher, H. Schumacher, and W. Menzel, "A compact ultra-wideband radar for medical applications," FREQUENZ, vol. 63, no. 1–2, pp. 1–8, Feb. 2009.
[4] X. Li, E. J. Bond, B. D. V. Veen, and S. C. Hagness, "An overview of ultra-wideband microwave imaging via space-time beamforming for early-stage breast-cancer detection," IEEE Trans. on AP, vol. 47, no. 1, pp. 19–34, Feb. 2005.

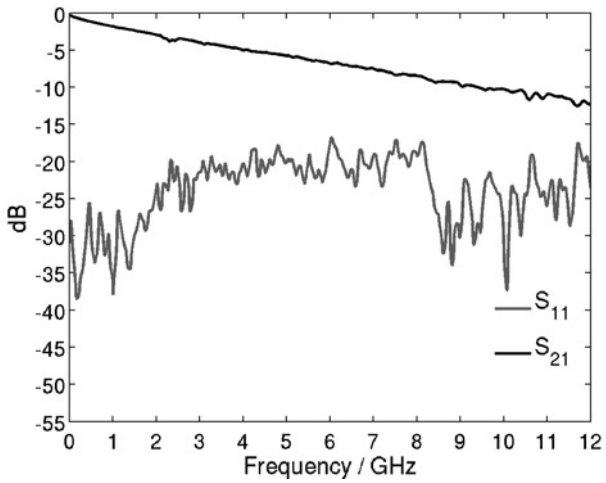

Fig. 9: Measured S-parameters of the triplate delay line.

[5] Federal Communications Commission, "Revision of part 15 of the commission's rules regarding ultra-wideband transmission systems", Washington D.C., USA, First Report & Order 48–02, Apr. 2002.
[6] T. Thiasiriphet and J. Lindner, "A Novel Comb Filter Based Receiver with Energy Detection for UWB Wireless Body Area Networks", IEEE Int. Symp. on Wireless Communication Systems (ISWCS), pp. 498–502, Oct. 2008.
[7] J. Dederer, B. Schleicher, F. A. T. Santos, A. Trasser and H. Schumacher, "FCC compliant 3.1–10.6 GHz UWB pulse radar using correlation detection", IEEE Int. Symp. on MTT, pp. 1471–1474, Jun. 2007.
[8] H. Sheng, P. Orlik, A. M. Haimovich, L. J. Cimini and J. Zhang, "On the spectral and power requirements for ultra-wideband transmission," IEEE Int. Conference on Communications, vol. 1, pp. 738–742, May 2003.
[9] A. Schüppen, J. Berntgen, P. Maier, M. Tortschanoff, W. Kraus and M. Averweg, "An 80 GHz SiGe production technology", III-Vs Review, vol. 14, pp. 42–46, Aug. 2001.

The authors would like to acknowledge Telefunken Semiconductor, Germany for providing the Si/SiGe library models and fabrication of the custom ICs and the German Research Foundation (DFG) for the funding within the priority programme UKoLoS.

Thanawat Thiasiriphet and Jürgen Lindner
Information Technology, Ulm University
Albert-Einstein-Allee 43, 89081 Ulm, Germany
E-mail: juergen.lindner@uni-ulm.de

Mario Leib and Wolfgang Menzel
Microwave Techniques, Ulm University
Albert-Einstein-Allee 41, 89081 Ulm, Germany
E-mail: wolfgang.menzel@uni-ulm.de

Dayang Lin, Bernd Schleicher and Hermann Schumacher
Electron Devices and Circuits, Ulm University
Albert-Einstein-Allee 45, 89081 Ulm, Germany
E-mail: hermann.schumacher@uni-ulm.de